Towards highly stable aqueous dispersions of multi-walled carbon nanotubes: the effect of oxygen plasma functionalization

Marta Garzia Trulli[1,6*], Eloisa Sardella[2,6*], Fabio Palumbo[2,6], Gerardo Palazzo[1,7], Lorena Carla Giannossa[3], Annarosa Mangone[1], Roberto Comparelli[4], Simone Musso[5], Pietro Favia[1,2,6]

[1] *Dipartimento di Chimica, Università degli Studi "Aldo Moro", via Orabona 4, Bari 70126, Italy*

[2] *CNR-NANOTEC, Istituto di Nanotecnologia, URT Bari c/o Dipartimento di Chimica, via Orabona 4, Bari 70126, Italy*

[3] *Dipartimento di Economia, Management e Diritto dell'Impresa, Università degli Studi "Aldo Moro", Largo Abbazia Santa Scolastica 53, Bari 70124, Italy*

[4] *CNR-IPCF, Istituto per i Processi Chimico-Fisici, U.O.S. Bari c/o Dipartimento di Chimica, via Orabona 4, Bari 70126, Italy*

[5] *Schlumberger-Doll Research Laboratory, 1 Hampshire St, Cambridge, Massachusetts 02139-1578, United States*

[6] *Consorzio INSTM, UdR Bari, Italy*

[7] *Center for Colloids and Surface Science - CSGI, RU Bari, Italy*

Abstract

Surface functionalization of multi-walled carbon nanotubes was carried out in oxygen-fed low-pressure plasma processes, in order to improve their dispersion in aqueous media. Differently from most papers in literature in this field, the plasma was switched on inside vials filled with the nanotubes, properly stirred during the process, in order to grant homogeneous functionalization. Different experimental variables were varied, including input power, treatment time and pressure, to investigate their influence on process efficiency. A detailed characterization of the plasma treated nanotubes, dry and in aqueous suspension, has been carried out with a multi-diagnostic analytical approach, to evaluate their surface chemical properties, morphology, structural integrity and stability in the colloidal state.

Keywords: multi walled carbon nanotubes (MWCNT); MWCNT functionalization; plasma functionalization; powders functionalization; colloidal stability; surface characterization.

*Corresponding authors.

Tel: +39-080-5443431. E-mail: marta.garziatrulli@uniba.it (Marta Garzia Trulli),

Tel: +39-080-5442295. E-mail: eloisa.sardella@cnr.it (Eloisa Sardella).

1. Introduction

Carbon nanotubes (CNTs) are an interesting molecular form of carbon belonging to the fullerene family, usually described as hollow tubular channels of one or more layers of graphene, denoted respectively as single wall (SWCNT) or multiwall (MWCNT). [1-3] Due to their unique mechanical, thermal and electronic properties, they are a promising material for a variety of potential applications. [2,4-6] CNTs have been proposed as filling and reinforcing nanoparticles in ceramic, polymer and cement matrices, for producing high-performance composite materials with superior mechanical, electrical, thermal and multifunctional properties [5,7-10] with respect to traditional reinforcing materials, like glass, carbon fibers or aluminum. [11,12] Because of their size (from one to tens of nm in diameter) and high aspect ratio (length-to-diameter ratio), CNTs can be distributed in a much finer scale than common fibers, leading to a more efficient crack bridging at the very preliminary stage of crack propagation within composites [12]. Furthermore, CNTs exhibit great mechanical properties and provide a large improvement in stiffness, strength and toughness which could be achieved simultaneously in the composite, because nanotubes deform before breaking. [13] However, to achieve this result, it is necessary to create strong bonds between the matrix and the nanotubes to transfer the load, an issue much more critical for CNTs than for carbon microfibers, because CNTs combine a large surface area with high chemical inertness. The van der Waals interaction between CNTs, coupled with an inhomogeneous dispersion in the matrix, causes the formation of large CNT aggregates that can easily initiate cracks rather than reinforce composites. [14,15] Therefore, a proper durable functionalization of CNTs is a prerequisite for their successful application in composites. Moreover, despite the peculiarities of CNTs, their low solubility in most solvents together with their weak affinity with most polymer matrices, mainly due to their hydrophobic and inert nature, greatly hinder their practical use in several fields of applications. [16] For these reasons, the chemical functionalization of nanotubes is widely studied; often it is achieved by means of oxidation via etching with inorganic acids. [17] Because of the harsh conditions of wet chemical methods, though, the structure of CNTs can be damaged, their length may be shortened and their peculiar properties can be compromised. [18]

Plasmas, ionized gases with equal density of positive and negative particles, can be ignited at very high (thermal plasmas, 10^3-10^4 K) or at room (cold, non equilibrium plasmas) temperature. Cold plasmas permeate today several industrial fields [19] for their ability to modify the surface composition and properties of materials with no alteration of the bulk, limited use of reagents, no use of solvents, dry technology, easy integration in industrial processes, and intrinsic sterility. Non-equilibrium plasma discharges can be ignited at low (LP, 1 - 100 Pa) or atmospheric (AP) pressure

by applying an alternated (kHz, MHz or MW) electrical field to a gas/vapor mixture in properly configured LP/AP plasma reactors, that can be accurately designed and optimized for processing small lab-scale samples or large-scale high throughput industrial products. By properly tuning parameters such as LP/AP regime, nature of the feed, reactor design, frequency power and modulation of the electric field, density and distribution of the active species (atoms, radicals, ions, electrons) generated in the plasma by the fragmented feed, as well as the interactions with the exposed substrates, can be properly tuned, making possible to tailor surface composition and properties of materials in many possible ways.

Three different surface modification plasma processes can be defined in general, namely: *Dry Etching*, where ablation reactions between the species generated in the plasma and a substrate form volatile products and modify at the micro/nano scale the morphology of the substrate, with or without the help of lithographic techniques; [20] *Plasma Enhanced Chemical Vapor Deposition (PE-CVD)* of thin coatings (1-10^3 nm) of many possible compositions, for an extremely wide range of properties that can be imparted at the surface of substrates (hardness, hydrophilic/phobic character, cytocompatibility, resistance to corrosion, etc.); [21] *Plasma Treatments*, where materials are exposed to cold plasmas fed with reactive (e.g., O_2, N_2, H_2, NH_3, H_2O vapor, etc.) or inert (Ar, He, etc.) non polymerizable gases. Plasma Treatments impart extremely shallow (a few nm) surface modifications, which include removal of surface contaminants, surface oxidation, and surface grafting of polar groups onto polymers to impart hydrophilic character, printability, affinity with other materials, anchor groups for (bio)molecules, cytocompatibility and other properties. [22]

Compared to the conventional wet-chemistry approaches, plasma treatments proved to be an appropriate technique for producing functionalized CNTs with minimal structural damage and superior properties (e.g. electrical), mainly due to the mild conditions applied, in terms of treatment time and temperature. [18,23] Furthermore, it is a flexible, timesaving and contaminant-free method, which allows tailoring of surface properties, without modifying the massive properties of the bulk. [22,24] The excited molecules and radicals, generated during the plasma discharge, attack the sp^2-hybridized graphite-like C=C bonds, creating open ends and defect sites acting as prime sites for functionalization. Various functional groups can be grafted at CNTs under a glow discharge, depending on the feed and on the experimental conditions. [23]

In the last few years several plasma sources have been utilized in different configurations and conditions for surface functionalization of carbon materials, including vertically-aligned CNT arrays and CNT films obtained by drop casting of powder/solvent suspensions. [25-29] Instead, the direct treatment of CNT powders is less studied, primarily because of the difficulty in handling them and in obtaining homogeneous modifications on a large scale. Most studies deal with the use

of plasma reactors without a suitable system for stirring the nanoparticles. Recently, for instance, MWCNTs have been functionalized with amine or carboxyl functional groups, by exposing them to He/NH_3 and humid air feeds, respectively, in an AP dielectric barrier discharge (DBD) reactor, in order to create compatible interfaces for enzyme immobilization. [30,31] Chen et al. [32] reported that amine-functionalized MWCNTs with higher selectivity for primary amines can be obtained with LP plasma treatments in N_2/H_2 mixtures, or by LP PE-CVD processes fed with heptylamine, thus improving their dispersion and the interfacial bonding with an epoxy resin. A plasma pre-treatment under N_2 was used to activate MWCNTs toward the polymerization of acrylic acid or the grafting of chitosan molecules, consequently enhancing their pre-concentration and immobilization capacity towards heavy metal ions for the abatementr of the environmental pollution. [33,34] Shi et al. [35] reported the plasma polymerization of styrene in radio frequency (RF) LP plasma source where MWCNTs were vigorously stirred during the treatment, so that their surface exposed to the plasma could be continuously and homogeneously renewed for a uniform deposition. The dispersion in water of MWCNTs was found improved when oxygen-containing functional groups were grafted on surfaces by microwave-excited LP plasma fed with Ar/H_2O blends. [36] Furthermore, an enhanced dispersion was observed also in the case of CNTs LP plasma treated capacitively coupled in RF (13.56 MHz) plasmas fed with O_2 and N_2. [37] Due to their high thermal conductivity, CNTs plasma-treated with O_2 and CH_4/O_2 mixtures can be used to prepare stable dispersions of CNTs in water for heat transfer nanofluids. Indeed, Kim et al. [38] reported that LP O_2 plasma treatments led to very hydrophilic CNTs and to stable CNT dispersions in water; surface structure changes and defects were noticed, though.

O_2 plasma treated carbon nanotubes have proved to be a promising material for a wide range of applications. Recently they have been used also to develop a sensitive and selective sensor for nitrogen dioxide in the ambient, [39] supports to disperse platinum–ruthenium nanoparticles catalysts [40] and as reinforcing fillers in polymers. [41] Coulombe developed a different method to obtain stable aqueous nanofluids, which consist on LP plasma treating CNTs grown directly on a stainless steel mesh, followed by their removal from the mash via ultrasonication in deionized water (DI). [42] Despite the above-cited studies, a full comprehension of the impact of plasma treatment on the dispersion stability of CNTs in water is still lacking.

In the present research, LP plasma processes were used to modify MWCNT powders, in order to increase their hydrophilic character and facilitate their dispersion in aqueous media generally used to manufacture MWCNT containing composites. In order to graft oxygen-containing groups, O_2 was selected as the gas feed. Several experimental parameters (including input power, time, and pressure) were varied in order to study their influence and optimize the process. Working on CNT

powders, stirred during the plasma treatment, allows to enhance the homogeneity of the functionalization at the whole CNT walls and reduce the anisotropic modification of the nanopowders, that generally occurs when plasma treatments are performed on CNTs deposited or grown directly on a substrate.

The aim of this work was to thoroughly investigate the physical-chemical properties and the colloidal stability of the plasma treated CNTs, correlating them with the different plasma parameters investigated. Moreover, the integrity of plasma treated MWCNTs was confirmed by TEM and Raman analysis. A deep characterization of the powders and of the suspensions in water of untreated (U-CNTs) and O_2 plasma treated samples (PT-CNTs) was performed. The behavior of MWCNTs dispersed in water was evaluated in terms of ability to disentangle the bundles and stability of the suspensions.

2. Materials and Methods

2.1 Substrate

Commercially available MWCNTs (Cheap Tubes Inc., Cambridge, USA) were used without further purification. They are 8-15 nm in diameter with a length of 10-50 μm. The choice of low price and low purity MWCNT was done thinking about a substrate that could be profitably used for low cost large-scale industrial applications (e.g. cementitious composites).

2.2 Reactor set-up and experimental plasma treatment conditions

The plasma functionalization of MWCNTs was carried out in a borosilicate glass tubular LP plasma reactor (3 cm dia, 118 cm long), shown schematically in Figure 1 and described in detail in [43]. The discharge was ignited by three external copper ring electrodes, two grounded and one connected to a 13.56 MHz RF power generator (RFX600, Advanced Energy). The impedance of the circuit was matched manually with that of the reactor by means of a homemade matching network. Samples were placed in the reactor in Pyrex vials (2.2 cm dia, 20 cm long) with a frosted Pyrex glass cap fitted with an opening (1 mm) wide enough to let the feed gas in contact with the sample, but small enough to limit the leakage of the CNTs under vacuum conditions. To increase the homogeneity of the plasma treatments, CNTs were stirred by intermittently rotating the vials with a magnet through a small ferromagnetic bar glued at the bottom of the vials. In these conditions, the discharge was localized within the vials, where up to 50 mg of CNTs were homogeneously treated in each batch. After a preliminary optimization study with different gases, O_2 (99.99%, Air Liquide)

was chosen as process gas at fixed flow rate of 15 sccm (electronic mass flow controllers, MKS). The effect of RF input power (20 – 100 W), treatment time (5 – 30 minutes) and pressure (150 – 600 mTorr) were evaluated individually, keeping constant the other parameters. The gas pressure in the chamber, served by a rotary pump (Pfeiffer), was monitored using a Baratron capacitance manometer (MKS 626, 1 Torr).

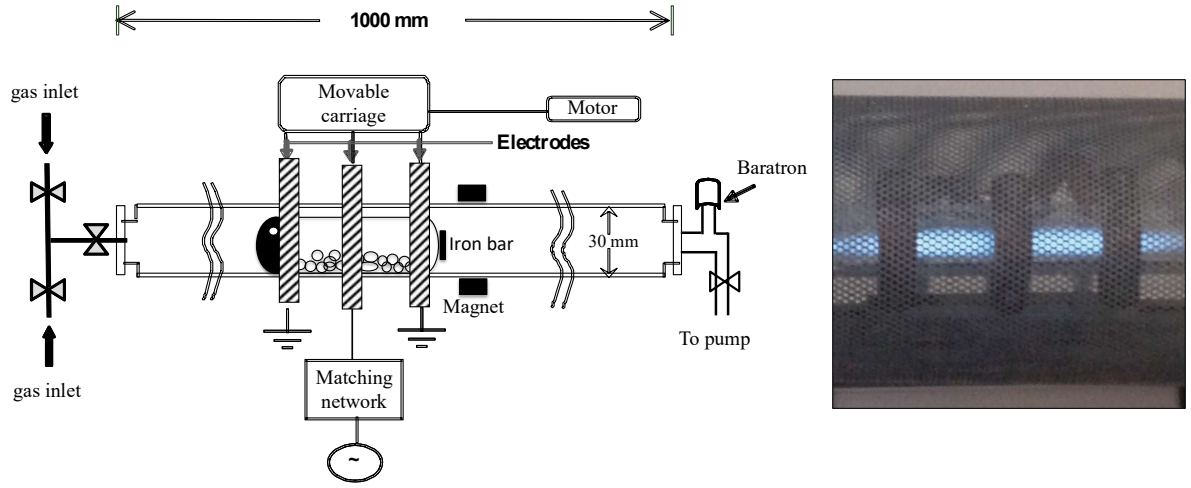

Figure 1: Scheme of the RF plasma reactor with rotating sample holder (left) and picture of the O_2 glow discharge localized in the Pyrex vial (right).

2.3 Chemical characterization of dry MWCNTs

X-ray Photoelectron Spectroscopy (XPS) was performed on powders gently pressed on a conductive adhesive aluminum tape. A Theta Probe Thermo VG Scientific XPS instrument (base pressure $1x10^{-9}$ mbar; monochromatic AlKα radiation, 1486.6 eV; 300 W; take-off angle 54.5°; 300 μm spot size) was used. Wide scan and high-resolution C1s and O1s spectra were acquired at 150 eV and 100 eV pass energy, respectively. Charging effects were compensated with a flood-gun (−1 eV electron energy, extraction potential 40 V). The aliphatic C1s component was used as binding energy (BE) reference at 284.8 ± 0.2 eV. Spectral data were processed with the Thermo Avantage software (v. 5.24, © 1999–2010 Thermo Fisher Scientific). Curve-fitting analysis was applied to all high-resolution spectra using a Smart type background and Gaussian/Lorentzian peak shapes.

MWCNTs were ground together with KBr powder (FT-IR grade, ≥ 99%, Sigma Aldrich), pressed into tablets (CNT/KBr 10^{-3}, w/w) and then analyzed by Fourier Transform Infrared (FT-IR) absorption spectroscopy under vacuum with a Vertex 70V Bruker spectrometer in transmission mode. Tabs were introduced into the sample compartment and evacuated at 1 Torr for 30 min.

The effects of plasma treatments on the graphitic lattice of MWCNTs was evaluated by Raman spectroscopy. A LabRAM HR Evolution – HORIBA instrument equipped with Nd:YAG (1064 nm), He-Ne (633 nm), Ar (488-514 nm) lasers was used to obtain micro-Raman spectra. Three

objectives 20X, 50X and 100X (Leica DMLM microscope) have been used. Calibration was carried out on Si(111) standard (520.5 cm^{-1}). Three different spots were analyzed on both U-CNTs and PT-CNTs samples using the same acquisition parameters: excitation wavelength 514.0 nm, incident laser power on the samples 2.0 mW, 100X objective, 5 scans, and 30 seconds accumulation. The baseline correction and the best fitting of the characteristic D and G peaks were carried out.

2.4 Morphological characterization of MWCNTs

Characterization of the morphology of MWCNTs was performed by means of field emission scanning electron microscopy (SEM-FEG, ZEISS SUPRA 40) and of transmission electron microscopy (TEM, JEOL 1011 operated at 100 kV).

SEM analysis of dry samples was carried out on MWCNTs stuck directly onto adhesive carbon tape. However, in order to evaluate any morphological changes of samples upon water dispersion, CNT-water suspensions were drop-casted onto silicon shards, then dried at room temperature overnight, and SEM analyzed.

Samples for TEM analysis have been prepared by dropping 5 µL of the water suspension of the MWCNTs onto carbon-coated copper grids then letting the solvent dry. For a statistical determination of the average MWCNT diameter, at least 100 measurements have been counted for each sample.

2.5 Characterization of MWCNT water suspensions

U-CNTs and PT-CNTs were dispersed in water (0.35 mg/ml) in order to carry out a detailed characterization of the suspension obtained. The suspensions was kept in ultrasonic bath at 130 W for 15 minutes to get better dispersion and assist the disentanglement of aggregates. SEM analyses of supernatants (data not reported) were carried out to rule out effects of sonication power and exposure time on the integrity of the material.

In order to get a quantitative assessment of the dispersion in water, Near-Infrared (NIR) Absorption measurements of suspension were carried out (Agilent 8453 diode array spectrophotometer). In the case of CNT colloidal dispersions, both light absorption and scattering contribute to the (apparent) absorbance were measured. However, while the molar absorptivity depends mainly on the chemical nature of the chromophore groups, the scattering efficiency depends strongly on the particle size and on the wavelength. To have a fair comparison between CNT samples with different size, absorbance measurements have been carried out in the NIR region, where the contribution of the scattering is almost negligible. The dispersion stability of MWCNTs

in water was also examined by measuring the absorbance intensity of the suspension at 850 nm at different settling times.

Nanosizer ZS (Malvern instruments) characterization was used for the determination of the zeta potential (electrophoretic light scattering, ELS) and of the size distribution (Dynamic Light Scattering, DLS) of dispersed MWCNTs. DLS measurements were performed in backscattering at fixed detector angle of 173° (NIBS™), while the zeta potential measurements were performed using forward scattering (17°) setup in capillary cells. DLS data were collected leaving the instrument free to optimize the instrumental parameters (attenuator, optics position and number of runs). Usually the time autocorrelation function (ACF) of scattered light intensity was the average of 10-12 consecutive runs of 10 s each. The size distribution by intensity of scattered light was recovered, using the software implemented by the manufacturer, by taking the inverse Laplace transform of the ACF and subsequent application of Stokes-Einstein equation, assuming the viscosity of the water solution at 25°C. To study the effect of the pH on the MWCNT's zeta potential, the pH of the CNT suspensions were adjusted to between 2 and 10, by addition of 0.5 M HCl and 0.1 M NaOH solutions. The hydrodynamic radius r_h was measured five minutes after the addition of the acid or of the base.

The total acid sites concentration on U-CNTs and PT-CNTs was assessed by means of acid–base titration. [44,45] 25 mg of MWCNTs were sonicated for 15 min in 25 ml of NaOH 0.1 M, the nanotubes were then removed by filtration with a 0.45 μm pore-sized filter and 25 ml HCl 0.1 M were added to the filtered solutions. Finally, the HCl excess was titrated with NaOH 0.1 M. The reproducibility of the results was verified replicating the titration process performed for each sample.

3. Results

3.1 Characterization of dry MWCNTs

XPS analysis reveals that the atomic percentage of oxygen for U-CNTs is 5%, whereas for the PT-CNTs the value increases up to 6-13%, depending on the experimental conditions.

The results in terms of atomic O/C ratios as a function of the plasma parameters investigated are shown in Table 1. The O/C ratio of the U-CNTs is 0.06 ± 0.01 and it reaches a maximum of 0.14 ± 0.01 for the PT-CNTs treated at the longest treatment time, at the highest pressure, or at the minimum input power. Increasing the treatment time from 5 to 30 minutes (40 W, 150 mTorr) proves that a longer plasma treatment enhances the exposure of the sample to the reactive oxygen species (atoms, excited molecules) produced in the plasma, hence improving the amount of oxygen

groups grafted to the sample. Furthermore, also when increasing the pressure from 150 to 600 mTorr (40 W, 15 min), the higher density of oxygen species generated enabled a better functionalization. Conversely, an increase of power seems to worsen the efficiency of the treatment. For instance, samples treated at 100 W (150 mTorr, 15 min) show a low O/C ratio of 0.06 ± 0.02, comparable to that of native CNTs. This phenomenon can be likely due to the increased importance, with power, of competing etching (C + O → CO; C + O_2* → CO_2, etc.) with respect to grafting processes. The etching continually renews the surface of the samples, leaving the PT-CNTs practically untreated.

Table 1: Chemical composition (O/C) and NIR absorbance values at 850 nm of untreated and plasma treated MWCNTs, with 15 sccm of O_2, as a function of the input power, treatment time and pressure. n.d.= not detected

Experimental conditions		**O/C values**	**Absorbance values (850 nm)**
Untreated		0.06 ± 0.01	0.080 ± 0.001
150 mTorr, 15 min	**20 W**	0.14 ± 0.01	0.91 ± 0.01
	40 W	0.11 ± 0.01	0.43 ± 0.01
	80 W	0.10 ± 0.03	n.d.
	100 W	0.06 ± 0.02	0.37 ± 0.01
150 mTorr, 40 W	**5 min**	0.11 ± 0.01	0.16 ± 0.01
	15 min	0.11 ± 0.01	0.43 ± 0.01
	30 min	0.14 ± 0.01	1.07 ± 0.01
15 min, 40 W	**150 mTorr**	0.11 ± 0.01	0.43 ± 0.01
	300 mTorr	0.12 ± 0.01	n.d.
	600 mTorr	0.14 ± 0.01	0.95 ± 0.02

The comparison of XPS C1s spectra acquired on PT-CNTs prepared at different RF power values (150 mTorr, 15 min) is shown in Figure 2, along with that of U-CNTs, reported as reference. Plasma treatments broaden the high BE region of the spectra acquired on PT-CNTs regardless of the plasma process applied. The broadening in the 286 – 288 eV range of C1s spectra is due to O-containing moieties (i.e. COC, COH, C=O, COOH, COOR), attesting the successful grafting of

such species on CNTs. The most evident variation is related to the carbonyl groups at 287.8 eV. As expected from the O/C ratios trend, the most significant increment in the high BE region appears for samples treated at lowest power (20 W), whereas this contribution decreases upon increasing the power, likely due to the increased effect of etching reactions, as explained earlier.

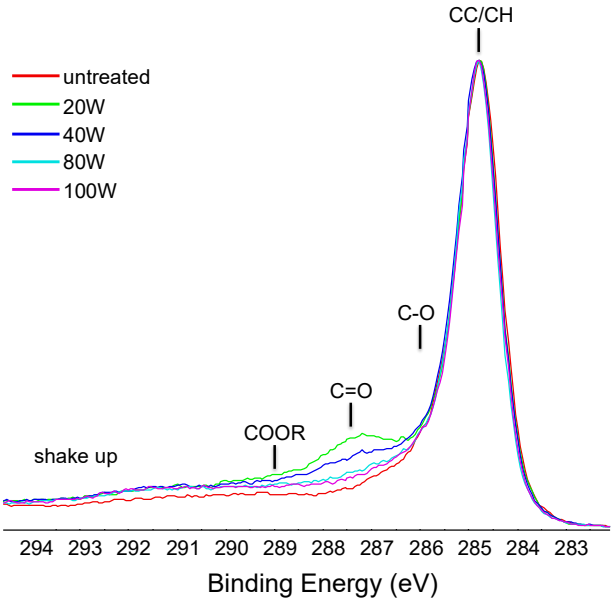

Figure 2: C1s spectra of U-CNTs (red line) and PT-CNTs (150 mTorr, 15 min) as a function of the input power (20 ÷ 100W).

FT-IR analysis allowed for the identification of chemical bonds and functional groups in the MWCNTs, confirming an overall increase of the density of O-containing functionalities after the treatments. Representative normalized adsorption FT-IR spectrum of a PT-CNT sample (40 W, 150 mTorr, 30 min) is shown in Figure 3, in comparison with the untreated one. The plasma treated sample exhibits an increment of the signal in the region relative to OH groups (3400 cm^{-1}) and a very broad peak around 1000 cm^{-1}, relative to CO single bond stretching. The signals around 1600 cm^{-1} could be due both to the formation of carbonyl species and to the formation of new C-C bonds due to chain rearrangement. Indeed, there are also absorption bands relative to C=O stretching (1723 cm^{-1}), due to acid groups, and C=C stretching (1630 cm^{-1}). Furthermore, the peak at 1577 cm^{-1} can be attributed both to the C-C and to COO^- stretching.

The SEM images of dried U-CNTs and PT-CNTs (40 W, 150 mTorr, 30 min) are presented in Figure 4. No major differences can be highlighted, indicating that the performed O_2 treatments result in negligible morphological changes.

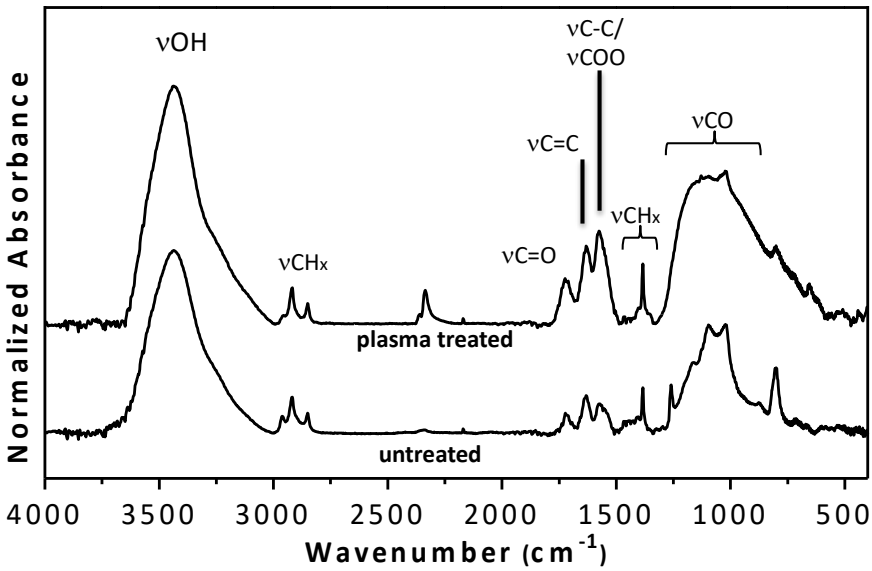

Figure 3: FT-IR spectra of U-CNTs and PT-CNTs (40 W, 150 mTorr, 30 min)

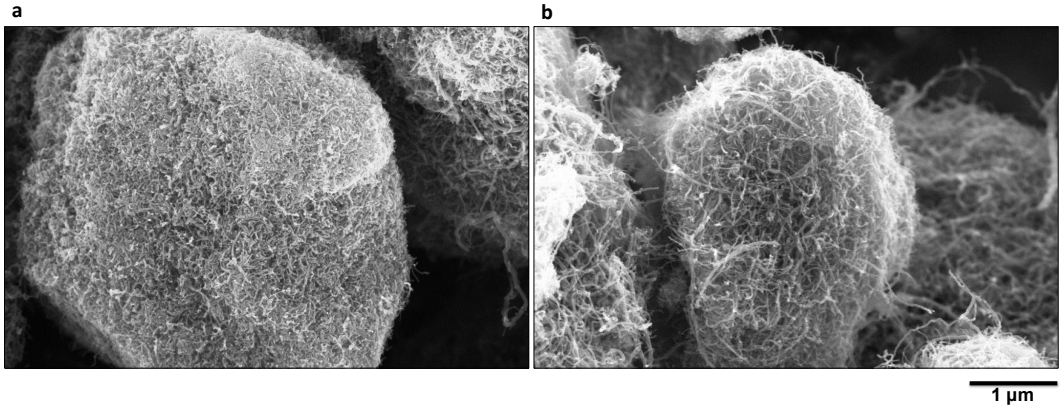

Figure 4: SEM image 50 Kx of dried MWCNTs. a: U-CNTs, b: PT-CNTs (40 W, 150 mTorr, 30 min)

3.2 Characterization of MWCNTs in aqueous suspensions.

PT-CNTs, dispersed in water and sonicated in an ultrasonic bath, were observed over time, in comparison with the untreated samples, in order to evaluate the efficiency of the dispersion and the stability of the resulting colloidal suspension. In Figure 5 (left) a picture of water dispersed U-CNTs and PT-CNTs (20 W, 150 mTorr, 15 min) is reported, after one month from the preparation of the suspension. It can be clearly observed how the functionalization with the O_2 plasma treatment increases the efficiency of the dispersion. PT-CNT dispersions remain stable for several months, while the untreated samples show precipitates even a few minutes after the sonication.

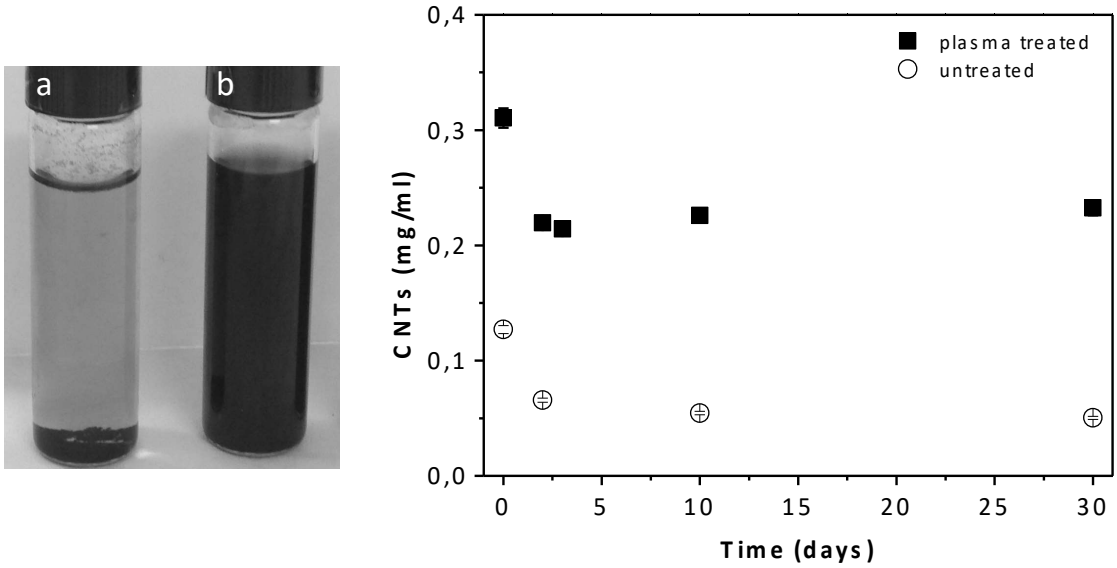

Figure 5: Picture (left) of U-CNTs (a) and of PT-CNTs (b) (40 W, 150 mTorr, 15min) dispersed in water, one month after the ultra-sonication. Dispersion stabilities (right) of U-CNTs and PT-CNTs (40 W, 150 mTorr, 15min) dispersed in DI water (0.35 mg/ml): Concentrations of the CNTs, calculated using NIR absorbance of the CNT suspension at wavelength of 850 nm, until 30 days settling time. This trend is representative for all the PT samples, whatever the experimental conditions used.

Since PT-CNT suspensions are so dark that it is difficult to check the presence of non-dispersed solid precipitate, as well as to obtain quantitative information on the CNT suspension, the stability of MWCNT/water dispersion was examined in detail carrying by means of NIR absorbance measurements at 850 nm at different settling times. The concentrations (mg/ml) of suspended CNTs were calculated using a calibration curve prepared by measuring the absorbance of water suspensions with known amount of CNTs a few seconds after the ultrasound treatment and vigorous shaking with a vortex-mixer. Figure 5 (right) shows dependence of the concentration on the settling time, where the zero time is measured immediately after the ultrasound-assisted dispersion in water. It can be seen that the concentration of the PT-CNTs dispersed in water has an abrupt drop (≈30%) within the first day, whereas it remains stable for at least one month afterward. U-CNTs, whose dispersion is only due to the sonication process, display a similar behavior, but their stable concentration is at least 80% lower than that of PT-CNTs. NIR absorption measurements of suspensions were carried out also to perform a more accurate comparison between the samples and get a quantitative assessment of the dispersion in water. The absorbance values are shown in Table 1. The colloidal stability of the PT-CNT dispersions follow the same trend of the O/C ratio, depending on the experimental conditions. Indeed, the highest absorbance values, indicating stable dispersions, can be observed with the increase of PT time and pressure, while a loss of stability is measured with the increment of power values.

Laser Doppler electrophoresis and dynamic light scattering measurements were carried out on

CNTs in solutions in order to obtain information about zeta potential and size distribution, respectively. In Figure 6 the zeta potential values of U-CNTs and PT-CNTs (20 W, 150 mTorr, 15 min) representative samples are plotted as a function of pH. It can be noted that the zeta potential becomes more negative with the increase of pH, reaching a constant value (-35 mV) between pH 5 and pH 8 for PT-CNTs. Moreover, at any pH-value, the zeta potential of PT-CNT is always much more negative than measured on U-CNTs.

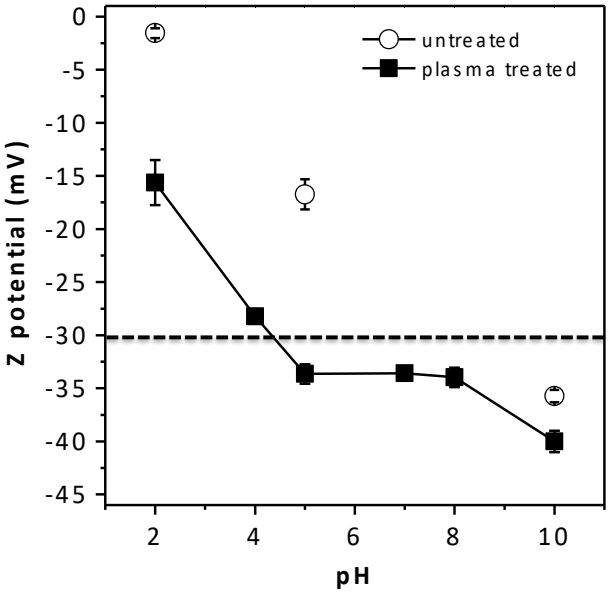

Figure 6: zeta potential as a function of dispersion pH for U-CNTs and PT-CNTs (20 W, 150 mTorr, 15 min) in water. The dotted line indicates the boundary between stable (z-pot < -30 mV) and unstable suspensions. This trend is representative for all the PT samples, whatever the experimental conditions used.

The values of zeta potential found on PT-CNTs can certainly be attributed to the presence of polar ionizable moieties, such as carboxylic functional groups, plasma-grafted at the surface of CNTs. Colloids with zeta potential values higher than +30 mV or more negative than -30 mV are normally considered stable, since they avoid coagulation by electrostatic repulsion, overcoming the van der Waals forces between particles. [46] Such a prediction should be taken with care, since it has been developed for homogenous spherical particles, nevertheless it can be suitable for a qualitative evaluation of the trends reported in Figure 6, attesting the high stability in water of PT-CNTs. This explains the different behavior observed in water for treated compared to untreated CNTs, which aggregate and precipitate. The quite negative zeta potential at pH 10 of U-CNTs could be due to the absorption of OH^- ions at their surface, as reported in literature. [47] Focusing the attention at pH 5, as shown in Figure 7, PT-CNTs exhibit zeta potential values more negative than U-CNTs and originate stable suspensions. However, no evident differences are observed between PT-CNTs produced in different conditions used. It can barely be noticed that the sample treated for

5 min presents the lower negative zeta potential value, confirming that shorter treatments are less effective.

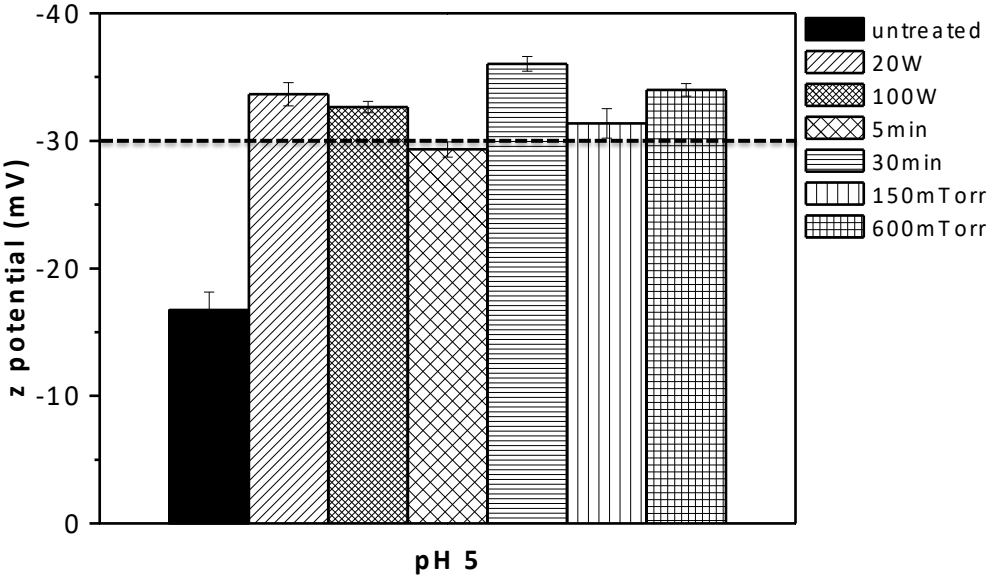

Figure 7: zeta potential values at pH 5 for U-CNTs and PT-CNTs (complete experimental conditions in Table 1) in water. The dotted line indicates the boundary between stable (z-pot < -30 mV) and unstable suspensions.

The concentration of the acid sites introduced on MWCNTs by O_2 plasma treatment can be determined by acid-base titration, carried out as described in the experimental section. Table 2 reports the concentration of acid sites evaluated for the PT-CNTs treated at 100 W (15 min, 150 mTorr) and at 600 mTorr (40 W, 15 min), namely those with the lowest and highest O/C values and dispersion behavior, respectively.

Table 2: Concentration of Acid Sites of U-CNTs and PT-CNTs

	Concentration of Acid Sites (mol %)
Untreated	1.6% ± 0.2
PT-CNTs 100 W (15min, 150mTorr)	2.9 % ± 0.4
PT- CNTs 600 mTorr (40W, 15min)	5.3 % ± 0.5

It can be observed that the mole percentage of acid sites (percentage of acid group moles per CNT mole) is increased by the plasma treatment with respect to native-CNT samples, in agreement with the zeta potential data. U-CNTs present a mole percentage of acid sites of about 1.6% (1.3 mmol/g), while PT-CNT sample present higher values. In particular, as expected, the 100W sample

presents a lower percentage (2.9 %) compared with the 600 mTorr sample, which shows a value of about 5.3 % (4.4 mmol/g). Interestingly, this increment of acid sites is higher with respect to the one found in literature for CNTs treated with conventional chemical methods. [48,49]

As mentioned before, DLS measurements can provide information about the size distribution of CNTs in solution.

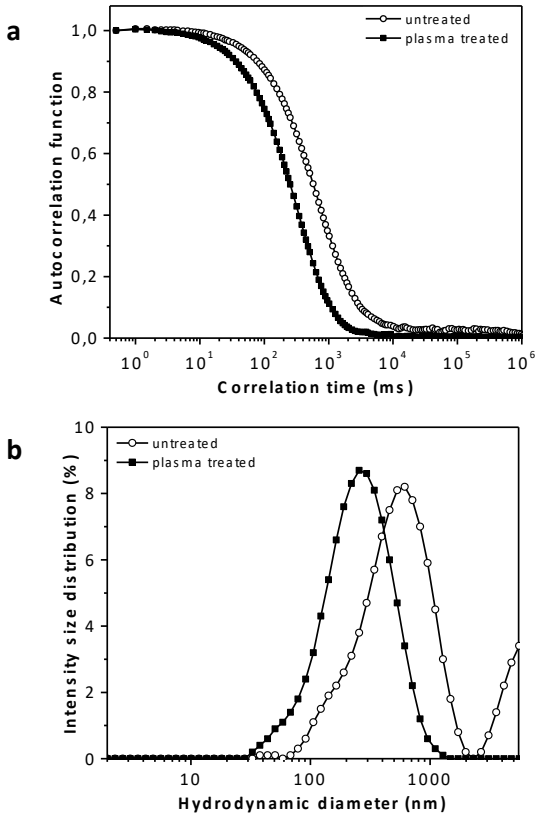

Figure 8: Autocorrelation function (a) and the intensity size distribution (b) for U-CNTs and PT-CNTs (20W, 150 mTorr, 15 min) dispersed in water at pH=5.

DLS measures time-dependent fluctuations in the light scattering intensity, arising from particles undergoing Brownian motion in solution. In Figure 8a the autocorrelation functions (ACF) of the scattered light for representative samples of U-CNTs and PT-CNTs (20 W, 150 mTorr, 15 min) dispersed in water are shown. The ACF of plasma treated samples decays at zero at shorter correlation time, compared with the ACF measured for U-CNTs. This is due to PT-CNTs dispersion in form of small fast-diffusing particles, while the untreated sample forms large slow-diffusing aggregates. It should be also noted that, in the case of U-CNTs, the ACF has a very slow phase that does not vanish in the hundreds of ms timescale, suggesting the presence of objects with sizes of tenths of microns. CNTs and their aggregates are, of course, intrinsically polydisperse in size and the easiest way to grasp such a spreading of dimensions is in term of the size intensity distribution.

This is the fraction of light scattered by particles of different size (strictly different hydrodynamic radius) and can be retrieved from the ACF, according to well assessed numerical methods. The intensity distribution functions for U-CNTs and PT-CNTs are shown in Figure 8b. It is evident that PT-CNTs have sizes distributed around 250 nm while the U-CNTs size-distribution has a maximum around 700 nm. In addition U-CNT have a non-negligible fraction of object with sizes above one μm (with the DLS equipment used size above 6 μm is not accessible). As a whole, the data of Figure 8 confirms the aggregation of U-CNTs in water and the disentanglement of the aggregates after the plasma treatments.

Usually, in literature, SEM analysis of modified CNTs is carried out onto dry treated samples. In this work, the morphology of CNTs was also characterized after their dispersion in water. This is important since, as shown in Figure 4, often no major differences are evidenced in the CNT bundles after the plasma treatment, if they are not dispersed in water.

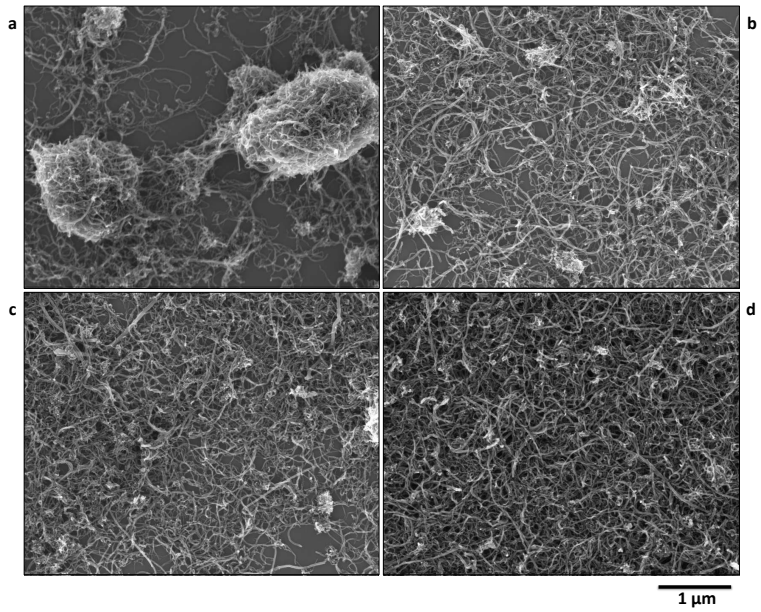

Figure 9: SEM image at 50000 x of dry MWCNTs collected after dispersion in water. a: U-CNTs, b: PT-CNTs (40 W, 5 min, 150 mTorr), c: PT-CNTs (40 W, 15 min, 600 mTorr), d: PT.CNTs (40 W, 30 min, 150 mTorr).

Figure 9 shows the SEM image of U-CNTs and PT-CNTs drop casted after dispersion in water. For the untreated sample (a) the presence of large compact bundles can be still observed. The similarity with the aggregates present in the pristine powder (see Figure 4) suggests that such aggregates are coils that have not been debundled in water. Plasma treated samples (b, c, d), instead, after the interaction with water show smaller compact coils, in agreement with the r_h data, as a result of the plasma functionalization processes. Furthermore, it can be noticed that in sample (b) treated for 5 min at 150 mTorr (40 W) still the presence of compact aggregates is visible, confirming that such treatment is less effective, for its short duration. On the contrary, increasing

the pressure at 600 mTorr (sample c) or the treatment time at 30 min (sample d), the amount of compact aggregates is drastically reduced. This reduction of number and size of compact coils is an interesting result with respect to the preparation of homogeneous CNT dispersions to be used for reinforcing composite materials.

3.3 Morphology and structural integrity of plasma treated MWCNTs

In order to get more insights on the morphology changes, TEM analyses were carried out on the samples treated in the more harsh conditions. TEM images of U-CNTs and PT-CNTs at the longest treatment time (40 W, 150 mTorr, 30 min), highest power (100 W, 150 mTorr, 15 min) and highest pressure (40 W, 600 mTorr, 15 min), are shown in Figure 10.

The analysis of the main diameter of the PT-CNT samples, reported in Table 3 in comparison with untreated ones, suggests that the plasma treatments do not significantly affect their structural morphology. It can be noticed that the sample treated at the highest power of 100 W presents the smallest diameter, however the difference is not so noticeable. This finding is in agreement with the fact that etching processes predominate at high power, that remove the grafted oxidized functionalities without thin excessively the samples.

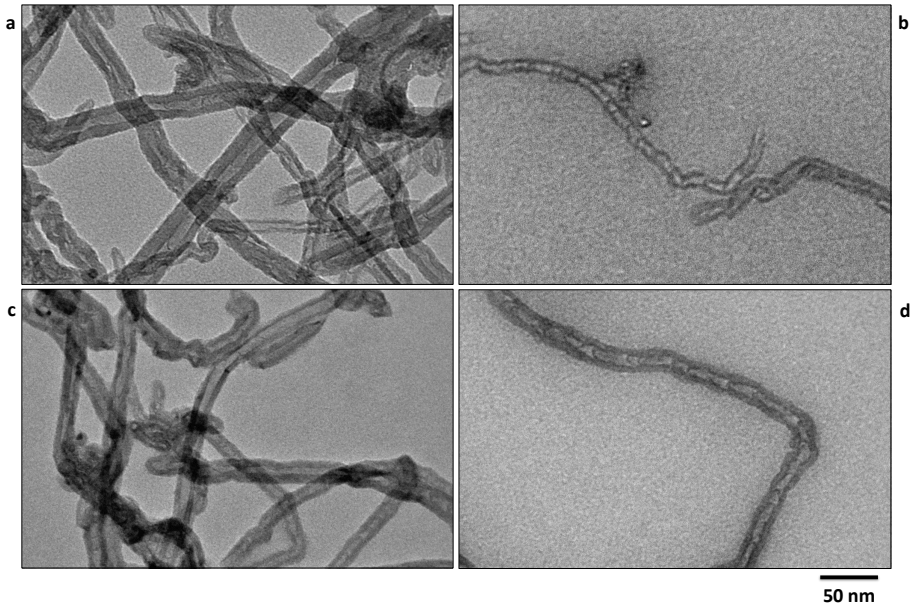

Figure 10: TEM images of water dispersed MWCNTs. a: U-CNTs, b: PT-CNTs (100 W, 15 min, 150 mTorr), c: PT-CNTs (40 W, 15 min, 600 mTorr), d: PT-CNTs (40 W, 30 min, 150 mTorr).

Table 3: Statistic distribution of U-CNTs and PT-CNTs diameters.

MWCNTs diameters (nm)	
Untreated	22 ± 3
PT-CNTs 600 mTorr (40 W, 15 min)	19 ± 2
PT-CNTs 30 min (40 W, 150 mTorr)	17 ± 3
PT-CNTs 100 W (150 mTorr, 15 min)	16 ± 3

More information about the purity, graphitic structure and defects of plasma treated and untreated MWCNTs was obtained from Raman spectroscopy. [50] Raman spectra of MWCNTs exhibit two main bands. [51,52] The peak around 1340 cm^{-1}, called the ‘‘D-band’’, is considered as a measure of ‘‘disorder’’ in the graphitic lattice in graphitic materials (A_1g mode). The G band, in the 1550-1600 cm^{-1} range, corresponds to the tangential vibrations of the carbon atoms (E_2g mode). This peak is a good mark of the graphitization of the sample. Second order bands can occur above 2600 cm-1. [53] Moreover, differently to SWCNTs and DWCNTs, MWCNTs do not exhibit any low-frequency signal (~200 cm-1). This peak, assigned to the A_1g symmetry Radial Breathing Mode (RBM), has a frequency that is inversely proportional to the tube diameter but cannot be detected when more than two walls are present. [51]

The I_D/I_G ratio between the intensity of the D and G bands is of particular interest, since it allows to evaluate the defects introduced in the graphitic lattice. [54] In fact, while the intensity of the G-band (I_G) does not depend on the lattice defect density, the D-band intensity I_D increases with the defect density. [55] Normalized spectra of U-CNTs and PT-CNTs are reported in Figure 11. It can be noted how the plasma treatment increases slightly the intensity of the D-band related to the induced disorder.

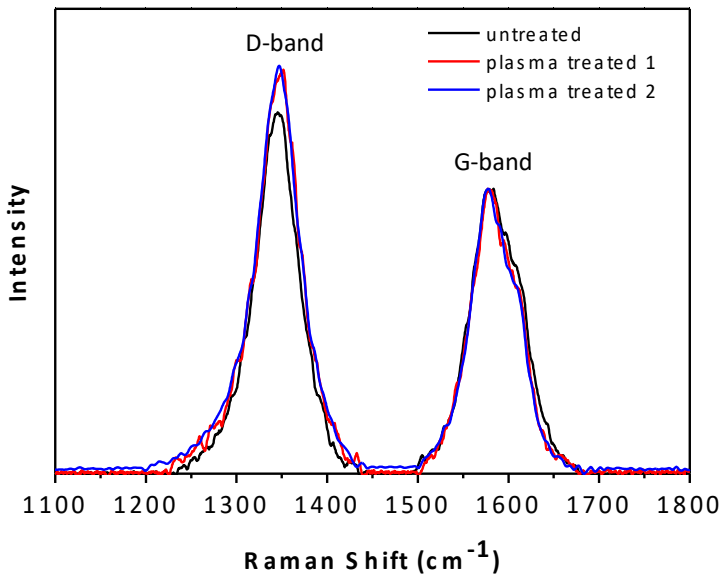

Figure 11: Normalized Raman spectra of U-CNTs, PT-CNTs 1 (40 W, 600 mTorr, 15 min) and PT-CNTs 2 (40 W, 150 mTorr, 30 min) Acquisition parameters: excitation wavelength: 514.0 nm, incident laser power on the samples < 2.0 mW, 100x objective, 5 scans (30 s each).

As reported in Table 4, the two plasma treated samples show similar I_D/I_G ratios, both higher than the untreated one. Since no relevant morphological changes were observed by electron microscopy after the O_2 plasma treatment, the slight increase in crystallinity defects revealed by Raman data can be attributed to the chemical functionalization of the material, as detected by other analyses.

Table 4: Raman spectroscopy data analysis of U-CNTs and PT-CNTs

Sample	**D-band (cm^{-1})**	**G-band (cm^{-1})**	**I_D/I_G**
Untreated	1350	1581	1.35
PT-CNTs **600 mTorr** (40 W, 15 min)	1347	1577	1.45
PT-CNTs **30 min** (40 W, 150 mTorr)	1346	1576	1.46

4. Conclusions

Oxygen low-pressure plasma processes described herein effectively tune the surface functionality of commercially available low cost multi-walled carbon nanotubes powder, by generation of surface oxygenated chemical groups. The treatment, whose efficiency was

demonstrated by chemical analyses, leads to a clear modification of the nanotubes. Their dispersion and stability in aqueous media is significantly improved due to the introduction of polar ionizable acid sites (highlighted by zeta potential analyses and acid-base titrations), preventing the agglomeration between adjacent nanotubes. The resulting dispersions of plasma treated nanotube powders in water remained stable for at least one month (i.e. about 70% of suspended particles), which is a highly significant property for their application in nanocomposite materials. In particular, this set of experiments in oxygen discharges has highlighted that the best results, in terms of dispersion properties and chemical surface functionalization, can be obtained at longest process times and at the highest pressure tested. Furthermore, it was confirmed that the enhanced dispersion was achieved in such mild conditions that the structural integrity of multi-walled carbon nanotubes is not affected.

Acknowledgements: Schlumberger-Doll, INSTM, CSGI and the projects LIPP (Rete di Laboratorio 51, Regione Puglia) and SISTEMA (PON "Laboratorio per lo Sviluppo Integrato delle Scienze e delle Tecnologie dei Materiali Avanzati e per dispositivi innovativi", MIUR) are gratefully acknowledged for funding and supporting this research. Mr. Savino Cosmai (CNR-NANOTEC) and Mr. Danilo Benedetti (Univ. Bari) are acknowledged for their technical contribution.

References

[1] S. Iijima. Helical microtubules of graphitic carbon. Nature 354 (1991) 56-58.
[2] M.F.L. De Volder, S.H. Tawfick, R.H. Baughman, A.J. Hart. Carbon Nanotubes: Present and Future Commercial Applications. Science 339 (2013) 535-539.
[3] V.N. Popov. Carbon nanotubes: properties and application. Materials Science and Engineering: R: Reports 43 (2004) 61-102.
[4] R.H. Baughman, A.A. Zakhidov, W.A. de Heer. Carbon nanotubes - the route toward applications. Science 297 (2002) 787-792.
[5] J.N. Coleman, U. Khan, W.J. Blau, Y.K. Gun'ko. Small but strong: a review of the mechanical properties of carbon nanotube–polymer composites. Carbon 44 (2006) 1624-1652.
[6] P. Sharma, N. Kumar Mehra, K. Jain, N.K. Jain. Biomedical applications of carbon nanotubes: a critical review. Current Drug Delivery 12 (2015).
[7] P.J.F. Harris. Carbon nanotube composites. International Materials Reviews 49 (1) (2004) 31-43.
[8] E.T. Thostenson, Z. Ren, T.W. Chou. Advances in the science and technology of carbon nanotubes and their composites: a review. Composites Science and Technology 61 (2001) 1899-1912.
[9] S.J. Chen, F.G. Collins, A.J.N. Macleod, Z. Pan, W.H. Duan, C.M. Wang. Carbon nanotube - cement composites: A retrospect. The IES Journal Part A: Civil & Structural Engineering 4 (4) (2011) 254–265.
[10] G. Ferro, J.M. Tulliani, S. Musso. Frattura ed Integrità Strutturale. 18 (2011) 34-44.

[11] O. Breuer, U. Sundararaj. Big Returns From Small Fibers: A Review of Polymer/Carbon Nanotube Composites. Polymer Composites 25 (6) (2004) 630-645.
[12] S. Musso, J.M. Tulliani, G. Ferro, A. Tagliaferro. Influence of carbon nanotubes structure on the mechanical behavior of cement composites. Composites Science and Technology 69 (2009) 1985-1990.
[13] L. Zajickovà, Z. Kucerovà, V. Bursıkovà, M. Eliàs, J. Houdkovà, P. Synek, H. Marsıkovà, O. Jasek, Carbon Nanotubes Functionalized in Oxygen and Water Low Pressure Discharges used as Reinforcement of Polyurethane Composites. Plasma Processes and Polymers 6 (2009) S864-S869.
[14] P.M. Ajayan, J.M. Tour. Nanotube composites. Nature 447 (2007) 447, 1066-1068.
[15] A.L. Mohd Tobi, I. Zaman, S. Jamian, A.E. Ismail, A review on carbon nanotubes reinforced ceramic composite. ARPN Journal of Engineering and Applied Sciences (2015).
[16] C. Chen, B. Liang, D. Lu, A. Ogino, X. Wang, M. Nagatsu. Amino group introduction onto multiwall carbon nanotubes by NH3/Ar plasma treatment. Carbon 48 (2010) 939-948.
[17] D. Tasis, N. Tagmatarchis, A. Bianco, M. Prato. Chemistry of Carbon Nanotubes. Chemical Reviews 106 (2006) 1105-1136.
[18] F.Pourfayaz, Y. Mortazavi, A.A. Khodadadi, S.H. Jafari, S. Boroun, M.V. Naseh. A comparison of effects of plasma and acid functionalizations on structure and electrical property of multi-wall carbon nanotubes. Applied Surface Science 295 (2014) 66-70.
[19] R. d'Agostino, P. Favia, C. Oehr, M.R. Wertheimer. Low-Temperature plasma processing of materials: Past, present, and future. Plasma Processes and Polymers 2 (2005) 7-15.
[20] V.M. Donnelly, A. Kornblit. Plasma etching: Yesterday, today, and tomorrow. Journal of Vacuum Science & Technology A 31 (2013).
[21] P. Favia. Plasma deposited coatings for biomedical materials and devices: fluorocarbon and PEO-like coatings. Surface and Coatings Technology 211 (2012) 50-56.
[22] P. Favia, N. DeVietro, R. DiMundo, F. Fracassi, R. d'Agostino. Tuning of acid/base surface character of carbonaceous materials by means of cold plasma treatments. Plasma Processes and Polymers 3 (2006) 66-74.
[23] M.V. Naseh, A.A. Khodadadi, Y. Mortazavi, F. Pourfayaz, O. Alizadeh, M. Maghrebi. Fast and clean functionalization of carbon nanotubes by dielectric barrier discharge plasma in air compared to acid treatment. Carbon 48 (2010) 1369-1379.
[24] Q. Chen, L. Dai, M. Gao, S. Huag, A. Mau. Plasma activation of carbon nanotubes for chemical modification. Journal of Physical Chemistry B 105 (3) (2001) 618-622.
[25] J.M. Tulliani, A. Cavalieri, S. Musso, E. Sardella, F. Geobaldo. Room temperature ammonia sensors based on zinc oxide and functionalized graphite and multi-walled carbon nanotubes. Sensors and Actuators B 152 (2011) 144-154.
[26] S. Yick, A. Mai-Prochnow, I. Levchenko, J. Fang, M.K. Bull, M. Bradbury, A. B. Murphy and K. K. Ostrikov, The effects of plasma treatment on bacterial biofilm formation on vertically-aligned carbon nanotube arrays. RSC Advances 5 (2015) 5142-5148.
[27] T. Abuzairi, M. Okada, Y. Mochizuki, N.R. Poespawati, R.W. Purnamaningsih, M. Nagatsu. Maskless functionalization of a carbon nanotube dot array biosensor using an ultrafine atmospheric pressure plasma jet. Carbon 89 (2015) 208-216.
[28] Z. Chen, X.J. Dai, K. Magniez, P.R. Lamb, D. Rubin de Celis Leal, B.L. Fox, X. Wang. Improving the mechanical properties of epoxy using multiwalled carbon nanotubes functionalized by a novel plasma treatment. Composites: Part A 45 (2013) 145-152.
[29] J. Lee, A. Efremov, R. Gang Son, S.P. Pack, H.W. Lee, K. Kim, K.H. Kwon. Ammonia-based plasma treatment of single-walled carbon nanotube thin films for bio-immobilization. Carbon 105 (2016) 430-437.
[30] Z. Rastian, A. A. Khodadadi, F. Vahabzadeh, C. Bortolini, M. Dong, Y. Mortazavi, A. Mogharei, M. V. Naseh, Z. Guob, Facile surface functionalization of multiwalled carbon nanotubes by soft dielectric barrier discharge plasma: Generate compatible interface for lipase immobilization. Biochemical Engineering Journal 90 (2014) 16-26.

[31] F. Khodadadei, H. Ghourchian, M. Soltanieh, M. Hosseinalipour, Y. Mortazavi. Rapid and clean amine functionalization of carbon nanotubes in adielectric barrier discharge reactor for biosensor development. Electrochimica Acta 115 (2014) 378-385.
[32] Z. Chen, X.J. Dai, P.R. Lamb, D.R. de Celis Leal, B.L. Fox, Y. Chen, J. du Plessis, M. Field, X. Wang, Practical Amine Functionalization of Multi-Walled Carbon Nanotubes for Effective Interfacial Bonding. Plasma Process and Polymer 9 (2012) 733-741.
[33] H. Cheng, J. Yu, K. Zeng, G. Hou. Application of Poly(Acrylic Acid)-Multiwalled Carbon Nanotube Composite for Enrichment of Rrace Hg(II). Plasma Process and Polymer (2013) DOI:10.1002/ppap.201300014.
[34] D. Shao, J. Hu, X. Wang. Plasma Induced Grafting Multiwalled Carbon Nanotube with Chitosan and Its Application for Removal of UO22+, Cu2+and Pb2+ from Aqueous Solutions. Plasma Process and Polymer 7 (2010) 977-985.
[35] D. Shi, P. He. Surface modifications of nanoparticles and nanotubes by plasma polymerization. Reviews on advanced materials science 7 (2004) 97-107.
[36] C. Chen, A. Ogino, X. Wang, M. Nagatsu. Oxygen functionalization of multiwall carbon nanotubes by Ar/H2O plasma treatment. Diamond & Related Materials 20 (2011) 153-156.
[37] L.G. Nair, A.S. Mahapatra, N. Gomathi, K. Joseph, S. Neogi, C.P. Reghunadan Nair. Radio frequency plasma mediated dry functionalization of multiwall carbon nanotube. Applied Surface Science 340 (2015) 64-71.
[38] Y.J. Kim, H. Ma, Q. Yu. Plasma nanocoated carbon nanotubes for heat transfer nanofluids. Nanotechnology 21 (2010) 295703 (7pp).
[39] P. Clément, A. Ramos, A. Lazaro, L. Molina-Luna, C. Bittencourt, D. Girbau, E. Llobet. Oxygen plasma treated carbon nanotubes for the wireless monitoring of nitrogen dioxide levels. Sensors and Actuators B 208 (2015) 444-449.
[40] R. Chetty, K.K. Maniam, W. Schuhmann, M. Muhler. Oxygen-Plasma-Functionalized Carbon Nanotubes as Supports for Platinum–Ruthenium Catalysts Applied in Electrochemical Methanol Oxidation, ChemPlusChem 80 (2015) 130-135.
[41] R. Scaffaro, A. Maio, S. Agnello, A. Glisenti. Plasma Functionalization of Multiwalled Carbon Nanotubes and Their Use in the Preparation of Nylon 6-Based Nanohybrids. Plasma Process and Polymer 9 (2012) 503-512.
[42] N. Hordy, S. Coulombe, J.L. Meunier. Plasma Functionalization of Carbon Nanotubes for the Synthesis of Stable Aqueous Nanofluids and Poly(vinyl alcohol) Nanocomposites. Plasma Process and Polymer 10 (2013) 110-118.
[43] E. Sardella, E.R. Fisher, J.C. Shearer, M. Garzia Trulli, R. Gristina, P. Favia. Plasma Process and Polymer 12 (8) (2015) 786-798.
[44] A.B. González-Guerrero, E. Mendoza, E. Pellicer, F. Alsina, C. Fernández-Sánchez, L.M. Lechuga. Discriminating the carboxylic groups from the total acidic sites in oxidized multi-wall carbon nanotubes by means of acid–base titration. Chemical Physics Letters 462 (2008) 256-259.
[45] Y.T. Shieh, G.L.Liu, H.H. Wu, C.C. Lee. Effects of polarity and pH on the solubility of acid-treated carbon nanotubes in different media. Carbon 45 (2007) 1880-1890
[46] P.C. Ma, N.a. Siddiqui, E. Mäder, J.-K. Kim, Correlation between electrokinetic potential, dispersibility, surface chemistry and energy of carbon nanotubes, Compos. Sci. Technol. 71 (2011) 1644–1651
[47] A. Schierz, H. Zanker. Aqueous suspensions of carbon nanotubes: Surface oxidation, colloidal stability and uranium sorption. Environmental Pollution 157 (2009) 1088-1094.
[48] H. Hu, A. Yu, E. Kim, B. Zhao, M.E. Itkis, E. Bekyarova, R.C. Haddon. Influence of the Zeta Potential on the Dispersability and Purification of Single-Walled Carbon Nanotubes. Journal of Physical Chemistry B 109 (2005) 11520-11524.
[49] V. Datsyuk, M. Kalyva, K. Papagelis, J. Parthenios, D. Tasis, A. Siokou, I. Kallitsis, C. Galiotis, Chemical oxidation of multiwalled carbon nanotubes, Carbon 46 (2008) 833-840.

[50] N. Chakrapani, S. Curran, B. Wei, P. Ajayan, A. Carrillo, R.S. Kane. Spectral fingerprinting of structural defects in plasma-treated carbon nanotubes. Journal of Materials Research 18 (10) (2003) 2515-2521.
[51] J.H. Lehman, M. Terrones, E. Mansfield, F.E. Hurst, V. Meunier. Evaluating the characteristics of multiwall carbon nanotubes Carbon 49 (8) (2011) 2581-2602.
[52] C. Annese, L. D'Accolti, G. Giambastiani, A. Mangone, A. Milella, G. Tuci, C. Fusco. Tunable Epoxidation of Single-Walled Carbon Nanotubes by Isolated Methyl(trifluoromethyl)dioxirane. European Journal of Organic Chemistry (2014) 1666–1671 DOI: 10.1002/ejoc.201301585.
[53] M.S. Dresselhaus, G. Dresselhaus, R. Saito, A. Jorio. Raman spectroscopy of carbon nanotubes. Physics Reports 409 (2) (2005) 47-99.
[54] S. Musso, M. Giorcelli, M. Pavese, S. Bianco, M. Rovere, A. Tagliaferro. Improving macroscopic physical and mechanical properties of thick layers of aligned multiwall carbon nanotubes by annealing treatment. Diamond and Related Materials 17 (2008) 542-547.
[55] Y.J. Lee. The second order Raman spectroscopy in carbon crystallinity. Journal of Nuclear Materials 325 (2004) 174-179.